HHS Public Access

Author manuscript

J Magn Reson. Author manuscript; available in PMC 2017 January 01.

Published in final edited form as:

J Magn Reson. 2016 January ; 262: 50–56. doi:10.1016/j.jmr.2015.12.005.

A bifunctional spin label reports the structural topology of phospholamban in magnetically-aligned bicelles

Jesse E. McCaffrey, **Zachary M. James**, **Bengt Svensson**, **Benjamin P. Binder**, and **David D. Thomas**

Department of Biochemistry, Molecular Biology, and Biophysics, University of Minnesota, Minneapolis, MN 55455, USA

Abstract

We have applied a bifunctional spin label and EPR spectroscopy to determine membrane protein structural topology in magnetically-aligned bicelles, using monomeric phospholamban (PLB) as a model system. Bicelles are a powerful tool for studying membrane proteins by NMR and EPR spectroscopies, where magnetic alignment yields topological constraints by resolving the anisotropic spectral properties of nuclear and electron spins. However, EPR bicelle studies are often hindered by the rotational mobility of monofunctional Cys-linked spin labels, which obscures their orientation relative to the protein backbone. The rigid and stereospecific TOAC label provides high orientational sensitivity but must be introduced via solid-phase peptide synthesis, precluding its use in large proteins. Here we show that a bifunctional methanethiosulfonate spin label attaches rigidly and stereospecifically to Cys residues at i and i + 4 positions along PLB's transmembrane helix, thus providing orientational resolution similar to that of TOAC, while being applicable to larger membrane proteins for which synthesis is impractical. Computational modeling and comparison with NMR data shows that these EPR experiments provide accurate information about helix tilt relative to the membrane normal, thus establishing a robust method for determining structural topology in large membrane proteins with a substantial advantage in sensitivity over NMR.

Graphical abstract

Corresponding Author: David D. Thomas, 321 Church St SE, Minneapolis, MN 55455 USA, Phone: (612) 625-0957, Fax: (612) 624-0632, ddt@umn.edu.

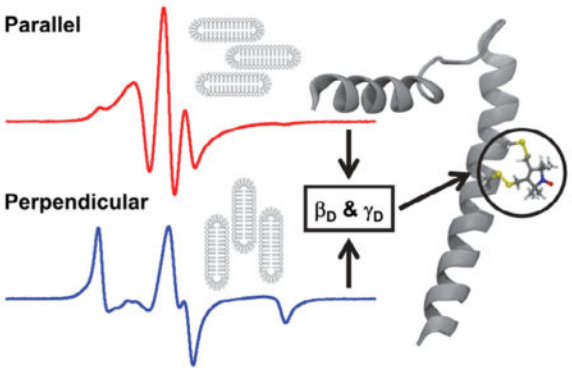

Keywords

bifunctional spin label; phospholamban; bicelles; orientation; EPR; molecular dynamics

1. Introduction

Magnetically-aligned bicelles are a powerful tool for studying the structural topology of integral membrane proteins by magnetic resonance spectroscopy. Reconstitution into aligned bicelles can resolve the anisotropic spectral properties of nuclei for NMR or nitroxide spin labels for EPR, yielding valuable information regarding protein orientation with respect to the bilayer. Bicelles (bilayered micelles) are mixtures of long- and short-chain phospholipids that combine to form flat patches of long-chain lipid bilayers bordered by the short-chain lipids [3]. Due to the negative magnetic susceptibility ($\Delta\chi$) of bicelles, at high magnetic field ($B_0 \geq 1$ T), they align spontaneously with the membrane normal (**n**) perpendicular to the field (**n** $\perp$ $\mathbf{B_0}$). Alignment is enhanced by the addition of lanthanides that associate with the bicelle surface and further decrease $\Delta\chi$ (Dy^{3+}), or increase $\Delta\chi$ (Tm^{3+}) to a positive value, flipping the bicelles such that they align with **n** parallel to the field (**n** $\|$ $\mathbf{B_0}$) [3].

In solid-state NMR spectroscopy, particularly $^{1}H/^{15}N$ PISEMA and SAMMY experiments, membrane protein alignment in bicelles (or mechanically-oriented bilayers) resolves $^{15}N - ^{1}H$ dipolar coupling and ^{15}N chemical shift anisotropies to permit the determination of transmembrane helical tilt and azimuthal rotation [4]. Similarly, membrane protein alignment in EPR can resolve the *g*-factor and hyperfine coupling anisotropies of nitroxides introduced via site-directed spin labeling, and optimization of long-chain lipid composition can produce excellent bicelle alignment in EPR, despite much lower magnetic field values than in NMR [5]. EPR offers a substantial advantage over NMR in sensitivity and can be applied to much larger proteins. However, conventional Cys-linked spin labels typically exhibit intrinsic sub-microsecond rotational mobility relative to the peptide backbone, resulting in motional averaging that limits their utility in EPR for determining peptide backbone orientation and rotational dynamics.

To provide accurate information about protein backbone rotational dynamics [6] and orientation of membrane proteins, we have used the spin label TOAC (2,2,6,6-

tetramethylpiperdine-1-oxyl-4-amino-4-carboxylic acid), which suppresses backbone-independent probe motion by incorporating the nitroxide group and α-carbon into the same six-membered ring [7]. Using TOAC, the nanosecond rotational rates and amplitudes of membrane protein domains have been measured by conventional EPR [6, 8–10], and even microsecond motions have been measured by saturation transfer EPR, enabling analysis of overall rotation of membrane proteins [11]. When applied to EPR in oriented bicelles, TOAC has been shown to enable accurate measurement of helix tilt relative to the membrane normal for small membrane proteins, including phospholamban (PLB) [7, 12], with results that are consistent with NMR and X-ray crystallography studies [1, 13, 14]. While the rigid and stereospecific attachment of TOAC affords high orientational resolution, TOAC must be introduced by solid-phase peptide synthesis, precluding its use in large proteins. Thus bicelle EPR studies using TOAC have focused exclusively on small (< 60 residues) proteins amenable to peptide synthesis [7, 15]. In the present study, we focus on an approach that is applicable to larger proteins, based on site-directed introduction of Cys residues.

The bifunctional spin label HO-1944 (Figure 1, BSL) is a derivative of the widely used monofunctional methanethiosulfonate spin label (MTSSL), and reacts with CxxC or CxxxC motifs along α-helices, or CxC motifs along β-sheets. As recently reviewed [16], this bifunctional attachment significantly restricts probe mobility and orientation with respect to the peptide backbone, typically producing stereospecific attachment that permits accurate EPR measurements of protein backbone dynamics and structure that are not feasible with MTSSL and other labels that react with single Cys residues. Studies using BSL have probed the μs–ms rotational dynamics (detected by saturation transfer EPR) of actin-bound myosin [17, 18] and tropomyosin [19], as well as the orientation of α helices within myosin in oriented muscle fibers [20, 21]. BSL has been shown to enhance the resolution of double electron-electron resonance (DEER) distance measurements for both aqueous [2] and membrane [22, 23] proteins, presumably due to restriction of the probe's attachment. In the present study, we demonstrate that BSL can be used, in conjunction with magnetically-aligned bicelles, to probe the structural topology of membrane proteins, with orientational resolution and accuracy comparable to those of TOAC. For our model system we chose phospholamban (PLB), a single-pass membrane protein that regulates the cardiac sarcoplasmic reticulum Ca-ATPase (SERCA) [24]. Wild-type PLB equilibrates between monomeric and homopentameric states, which possess different transmembrane helix tilts (21° vs 15°, respectively) [1, 25]. The fully functional monomeric mutant C36A/C41F/C46A (AFA) was employed to simplify the system and eliminate potential spin-spin interactions [26]. The structural topology of AFA-PLB in mechanically-oriented bilayers has been thoroughly characterized by hybrid solution/solid-state NMR techniques, permitting the interpretation of our results in the context of a high-resolution structure [1, 26, 27].

2. Materials and methods

2.1. Protein preparation and labeling

Single-Cys (F32C, for monofunctional labeling) and double-Cys (F32C/A36C, for bifunctional labeling) PLB constructs were prepared by QuikChange mutagenesis (Agilent

Technologies) of a plasmid encoding Cys-free (C36A/C41F/C46A) PLB as a cleavable fusion to maltose binding protein (MBP) [28]. Expression was carried out in BL21(DE3) cells (Lucigen) grown in Terrific Broth at 37 °C and induced with 0.5 mM IPTG once OD_{600} reached 2.5 – 3.0. Following induction, cells were incubated 20 hr at room-temperature before collection by centrifugation, after which expressed MBP-PLB was purified by amylose resin chromatography, cleaved with recombinant TEV protease [29], and purified by HPLC [30, 31]. Each purified, lyophilized PLB construct was solubilized at 100 μM in 50 mM Tris-HCl, 5% (w/v) SDS, pH 7.5 and immediately combined with 2-fold molar excess BSL (Toronto Research Chemicals) from a 25 mM stock in N,N-dimethylformamide, followed by 16 hr incubation at room-temperature with protection from light. The next day, spin-labeled protein was re-purified by HPLC and lyophilized, then solubilized at ~1 mg/mL in trifluoroethanol and stored at −20 °C.

Labeling stoichiometry was determined to be 0.95–1.0 (mol BSL/mol PLB), by dissolving a portion of each lyophilized powder in 5% (w/v) SDS and comparing the double integrals of their EPR spectra to that of a 100 μM TEMPOL standard, followed by determination of protein concentration using the BCA assay (Thermo Fisher Scientific). Stoichiometry was confirmed by electrospray ionization mass spectrometry (ESI-MS). Lyophilized powders were solubilized in 50:50 H_2O/acetonitrile (v/v) containing 0.1% (v/v) mass-spectrometry-grade formic acid (Sigma-Aldrich). Samples were characterized by direct infusion onto an Agilent MSD SL Ion Trap operating in positive ion mode.

2.2. Sample preparation and EPR spectroscopy

Spin-labeled PLB was reconstituted at 1400 long-chain lipids per PLB into 2/2/1 (mol/mol) DMPC (1,2-dimyristoyl-sn-glycero-3-phosphocholine, 14:0 PC) / POPC (1-palmitoyl-2-oleoyl-sn-glycero-3-phosphocholine, 16:0–18:1 PC) / DHexPC (1,2-dihexanoyl-sn-glycero-3-phosphocholine, 6:0 PC) bicelles containing 13% cholesterol (mol/mol long-chain phospholipid) and 20% $TmCl_3$ or $DyCl_3$ (mol/mol long-chain phospholipid) [5, 7, 32]. This lipid composition was shown previously to optimize bicelle orientation at X-band magnetic field strength and 298 K [5]. To prepare bicelles, lipid and cholesterol stocks in chloroform (Avanti Lipids) were combined with PLB, dried under N_2 gas, and stored overnight in a vacuum desiccator. The resulting films were resuspended at 25% (w/v) in 100 mM HEPES, pH 7.0 by thorough vortexing and ice bath sonication, after which the samples were combined with lanthanides also dissolved in 100 mM HEPES. Samples were then flash-frozen and thawed three times to ensure lipid homogeneity. To produce isotropic lipid vesicles, samples were prepared as described above while omitting DHexPC.

EPR experiments were performed on a Bruker EleXsys E500 spectrometer equipped with a resonator (ER 4122 SHQ) containing a quartz dewar insert attached to a nitrogen gas temperature controller. 16 μL samples were loaded into 0.6 mm inner diameter glass capillaries (Vitrocom) and plugged with Critoseal (Krackeler Scientific). For vesicle samples, spectra were acquired immediately at 298 K or 200 K. For alignment, bicelle samples were first incubated in the resonator for 5 min at 273 K in the absence of a magnetic field. The field strength was then raised to 1.1 T and the temperature gradually increased to 298 K at a rate of 2 K per minute. Samples were then incubated for 20 min at 298 K and 1.1

T before the field strength was decreased for EPR measurements [5]. Spectra at 298 K were acquired using 1 G peak-to-peak amplitude modulation, 5 mW microwave power, and a 120 G sweep width, while spectra at 200 K were acquired using 1 G peak-to-peak amplitude modulation, 0.1 mW microwave power and a 120 G sweep width.

2.3. Molecular dynamics simulations

To extract the helical tilt of PLB's transmembrane helix from EPR measurements, we modeled BSL at positions 32 and 36 of the PLB TM helix (residues Gln23 to Leu52) using the high-resolution NMR structure of AFA-PLB (PDB 2KB7) [34] and dihedral angles measured from the crystal structure of BSL-T4-lysozyme [2]. Langevin dynamics, with SCPISM implicit solvation at 300 K with a viscosity factor of 5 for enhanced sampling, was performed using CHARMM (CHARMM36 force field) [35, 36]. This method samples the conformational space efficiently without the long simulation times required by all-atom molecular dynamics simulations. During the 160 ns simulation, the backbone of the PLB helix was constrained to the initial conformation. From this trajectory, the probability distributions for the spherical angles describing the orientation of the PLB TM helix in the nitroxide probe frame (θ_{hp} and φ_{hp}, Figure 2b) were tabulated. These distributions were well-fit by a standard Gaussian model.

2.4. Data analysis

EPR spectra were background-corrected and normalized in WACY, an in-house EPR analysis program developed by Edmund Howard. WACY was also used to analyze the rigid-limit spectra acquired at 200 K. All other spectra were analyzed first using the LabView program MultiComponent [37] to determine approximate values for fitting parameters. These values were then refined using NLSL [38]. Spectra of randomly oriented samples were analyzed assuming the microscopic-order macroscopic-disorder (MOMD) model [38]. Initial values for the electron *g* and hyperfine tensors were obtained from fits to the EPR spectrum of a frozen (200 K) lipid vesicle sample. Spectra of aligned bicelles (parallel and perpendicular to the magnetic field) were fit globally under a partial MOMD model with the orienting potential provided by the lipid environment, with the director Ψ collinear with the membrane normal. We again used an isotropic rotational diffusion tensor and the first coefficient of the orienting potential (c_{20}). To optimize the fit, values for the *g*-tensor and axially symmetric hyperfine tensor were allowed to vary by no more than 1% and 5% respectively to account for changes in environmental conditions such as polarity. During global fitting, the director tilt angles were fixed at 0° (parallel) and 90° (perpendicular) while the diffusion tilt angles β_D and γ_D (Figure 2f) for the spin probe were allowed to vary. Parameter errors were estimated from at least four unique fitting routines per fit with differing starting conditions, as well as direct error output from MultiComponent and NLSL.

The PLB helix tilt angle θ_{nh} (Figure 2d) was defined as the dot product of the membrane normal ***n*** and the helix vector ***h*** in the nitroxide probe frame. The helix vector is described by angles θ_{hp} and φ_{hp} (Figure 2b), as determined from molecular dynamics simulations. To obtain the membrane normal ***n*** in the nitroxide probe frame, we started with its representation in the diffusion frame, which is simply the z-vector: (0, 0, 1). We then

performed an Euler rotation transformation (z-y-z convention, Figure 2f) using the diffusion tilt angles β_D and γ_D:

$$R=\begin{bmatrix} \cos(\beta_D)\cos(\gamma_D) & -\cos(\beta_D)\sin(\gamma_D) & \sin(\beta_D) \\ \sin(\gamma_D) & \cos(\beta_D)\cos(\gamma_D) & 0 \\ -\sin(\beta_D)\cos(\gamma_D) & \sin(\beta_D)\sin(\gamma_D) & \cos(\beta_D) \end{bmatrix} \quad (1)$$

Multiplication of the z-vector with *R* from Equation 1 yields the membrane normal in the nitroxide probe frame (***n*** in Figure 2a). Subsequently, the dot product was calculated to determine θ_{nh} (Figure 2d):

$$\theta_{nh}=\arccos(n\cdot h)$$
$$=\arccos\left\{\left(R\begin{bmatrix}0\\0\\1\end{bmatrix}\right)\cdot\begin{bmatrix}\sin(\theta_{hp})\cos(\phi_{hp})\\ \sin(\theta_{hp})\sin(\phi_{hp})\\ \cos(\theta_{hp})\end{bmatrix}\right\} \quad (2)$$

3. Results

3.1. Protein characterization by mass spectrometry

Electrospray ionization (ESI) mass spectrometry shows that the 32-BSL-PLB construct has one monofunctionally attached BSL with its second methanethiosulfonate group intact (Figure S1a), while 32/36-BSL-PLB contains a bifunctionally-attached label as the predominant species (Figure S1b). This is further supported by the absence of dipolar broadening in the EPR spectra (Figure 3), which would be observed clearly if two labels were each monofunctionally attached to the 32/36-BSL-PLB construct. Figure S1 also shows that PLB was not cross-linked by BSL for either of the 32- or 32/36-BSL-PLB constructs, as evidenced by the lack of higher molecular weight species.

3.2. EPR of randomly oriented membranes

To obtain initial values for the electron *g* and hyperfine tensors, we acquired the spectrum of monofunctional 32- and bifunctional 32/36-BSL-PLB in frozen lipid vesicles at 200 K and analyzed the spectra assuming a rigid-limit model with random orientation (Figure 3a,c). These frozen isotropic samples lack the confounding effects of rotational motion and anisotropy. The *g*- and *A*-tensor values are similar for monofunctionally and bifunctionally attached BSL (Table 1).

Spectra obtained at ambient temperature (298 K, Figure 3b,d) have the characteristic lineshape of strongly immobilized spin labels, and are only slightly narrower than those of frozen samples (Figure 3a,c), indicating that any nanosecond rotational motion is slow (τ_R > 10 ns) and/or restricted (order parameter S > 0.3). This is confirmed by analysis of rotational dynamics using a standard MOMD model (Table 1) [38]. Monofunctionally-labeled PLB is characterized by moderately slow (τ_R = 16.7 ± 1.1 ns) and restricted (S = 0.37 ± 0.09) rotational dynamics, compared with much slower (τ_R = 76.2 ± 2.2 ns) and more restricted (S = 0.55 ± 0.07) rotational dynamics for bifunctionally-labeled PLB.

3.3. EPR of aligned bicelles

To prepare aligned samples, we prepared 2:2:1 (mol/mol) POPC/DMPC/DHexPC bicelles containing 13% cholesterol (mol/mol long-chain lipid). With the addition of lanthanides (20% $TmCl_3$ or $DyCl_3$, mol/mol long-chain lipid), we observed complete alignment of these bicelles at 298 K using 5-DOXYL-stearic acid as a reporter (Figure S2) [5]. Spectra of bicelles with the membrane normal aligned parallel (**n** || $\mathbf{B_0}$) and perpendicular (**n** ⊥ $\mathbf{B_0}$) to the field show substantial differences in outer splitting (Figure S2), clearly indicating alignment. In contrast to the spectra of randomly oriented samples (Figure 3), spectra of aligned bicelles (Figure 4) are quite different for monofunctional and bifunctional labeling. For the monofunctionally attached 32-BSL-PLB, the spectrum of bicelles aligned parallel to the field has broadened features at low and high field (Figure 4a), indicating orientational disorder and/or sub-microsecond rotational dynamics. The corresponding spectrum of bicelles aligned perpendicular to the field (Figure 4b) is only slightly different from the spectrum of randomly oriented membranes (Figure 3b), also supporting orientational disorder. Since these bicelles are homogeneously aligned (Figure S2) and do not exhibit significant spin-spin interactions (Figure 3), Figure 4a,b indicates substantial disorder in the orientation of BSL relative to PLB in the monofunctionally-labeled construct. In contrast, the bicelle spectra from bifunctionally-labeled 32/36-BSL-PLB (Figure 4c,d) are quite distinct from each other and from the spectra of randomly oriented membranes (Figure 3d). Thus bifunctional labeling results in much greater dependence of the spectrum on bicelle orientation, indicating much greater alignment of the spin label relative to the membrane.

Based on the crystal structure of bifunctionally labeled BSL-T4-lysozyme [2] and previous EPR measurements of bifunctionally-labeled BSL-myosin in oriented muscle fibers [21], BSL is predicted to attach with its principal axis ($\mathbf{z_P}$) tilted ~75° relative to the helix long axis **h**. For PLB in bicelles aligned parallel to the field, **h** is only ~20° away from the membrane normal [1], which explains why bicelles aligned perpendicular to the field yield a spectrum with substantially wider splitting than for the parallel case (Figure 4a,c).

As in randomly oriented samples (Figure 3), 32-BSL-PLB in oriented bicelles is characterized by faster dynamics (shorter correlation time τ_R) with larger amplitude (lower order parameter S) (τ_R = 10.8 ± 0.8 ns, S = 0.39 ± 0.04) in comparison to 32/36-BSL-PLB (τ_R = 70.5 ± 4.1 ns, S = 0.57 ± 0.05) (Table 1). For 32-BSL-PLB, the nitroxide angles relative to the membrane normal are 62° ± 19° for β_D (tilt) and 48° ± 34° for γ_D (twist). The large uncertainties for monofunctionally attached BSL are consistent with substantial orientational disorder. In contrast, these angles are much better defined for 32/36-BSL-PLB (90° ± 3° for β_D and 62° ± 20° for γ_D, Table 1).

3.4. Molecular modeling and MD simulations

We found the position and orientation of BSL to be quite stable relative to the helix axis (**h**, Figure 2b), with our simulation reporting an average probe-to-helix polar angle (θ_{hp}) of 69° ± 3° (FWHM ~ 15°) and an average probe-to-helix azimuthal angle (φ_{hp}) of 71° ± 5° (FWHM ~ 20°) as shown in Figure 5. By calculating the dot product of the membrane normal and the helix axis (**n•h**) using the diffusion tilt angles corresponding to 32/36-BSL-PLB from Table 1 and the probe-to-helix angle distributions from Figure 5 (Equations 1 and

2), we obtained a PLB TM helix tilt of 21.8° ± 2° (Table 2), in excellent agreement with the helix tilt of 21° ± 2° determined by NMR [1]. When the simulated 32/36-BSL-PLB TM helix was aligned at the same orientation as the 2KB7 NMR structure in a lipid bilayer, we measured a probe-to-membrane angle of 89° ± 2° between the membrane normal and the nitroxide principal axis (Table 2). This is in excellent agreement with the value of β_D (90.0° ± 3°) from our fitted EPR data, since the director axis was taken to be the membrane normal ($\Psi = 0°$).

4. Discussion

Due to multiple possible labeling outcomes (monofunctional attachment, bifunctional attachment, cross-linking, etc), we characterized labeling for both 32-BSL-PLB and 32/36-BSL-PLB constructs by mass spectrometry. The results (Figure S1) show that under appropriate labeling conditions, bifunctional attachment can be obtained for a double-Cys target, as opposed to one or two monofunctional attachments. The label:protein molar ratio is an important consideration during sample preparation; we found that a 2:1 BSL-to-PLB molar ratio resulted in optimal labeling, as judged by immobilization and minimal free label (Figure S3). These results are specific to our protein constructs and labeling scheme. Thus, solubilization detergent, spin label concentration, labeling duration, and incubation temperature may all require optimization for specific applications.

Spectra of randomly oriented membranes show only slight differences due to monofunctional and bifunctional labeling (Figure 3), indicating that the probe is “strongly immobilized” ($\tau_R > 10$ ns and/or $S > 0.3$) in both cases. The strong immobilization of monofunctionally attached BSL is much greater than that typically observed for the monofunctional methanethiosulfonate spin label (MTSSL) [21]. This suggests that the second, unreacted methanethiosulfonate group of monofunctionally-attached BSL interacts with the protein and thus restricts probe mobility, as observed previously for a study of T4 lysozyme using 4-substituted MTSSL derivatives [39]. Computational analysis of spectra in Figure 3 reveals that bifunctional attachment of BSL to PLB yields significantly stronger immobilization (longer values of Table 2), similar to that of TOAC [11], showing that any nanosecond rotational motion of bifunctionally-labeled PLB at ambient temperature reflects that of the protein backbone of PLB. The difference between monofunctional and bifunctional attachment of BSL is clearly revealed by spectra of oriented bicelles, where spectra reveal much greater orientational order for bifunctional attachment (Figure 4), confirming the rigid and stereospecific attachment of BSL to the protein’s helical backbone.

The agreement between our EPR and MD data indicates that suitable analysis models were implemented in our study. The diffusion tilt angle β_D is directly calculable from both EPR and MD methods (Table 2), showing excellent agreement. In addition, our MD simulation of BSL on PLB is largely consistent with a previous X-ray crystal structure [2] (Table 2). Some deviation is expected due to differences in probe environment and local dynamics, as BSL is located near a loop region in the crystal structure [2], and at the center of a stable α-helix on our PLB construct. Perhaps most important is the agreement of the PLB TM helix tilt angle (Table 2) calculated from our EPR and MD measurements versus previous NMR

experiments [1]. This helps to validate our experimental approach of using oriented bicelle EPR in conjunction with MD simulations to determine protein topology.

5. Conclusions

We have shown that EPR spectra of a bifunctional methanethiosulfonate spin label (BSL, attached to two Cys side-chains separated by four residues) can be used to determine accurately the orientation and rotational dynamics of an α-helical segment of an integral membrane protein that is reconstituted into magnetically-aligned bicelles. A monofunctionally attached spin label cannot provide this accuracy. Thus BSL is a suitable alternative for the rigid and stereospecific spin label TOAC for large proteins where peptide synthesis is not feasible. This work substantially expands the range of proteins for which EPR can provide accurate information about orientation and rotational dynamics of structural elements.

Supplementary Material

Refer to Web version on PubMed Central for supplementary material.

Acknowledgments

This work was supported in part by National Institutes of Health grants GM27906, AR057220, and AR007612. EPR experiments were performed at the Biophysical Technology Center, University of Minnesota. We thank Octavian Cornea for assistance with preparation of the manuscript.

References

1. Traaseth NJ, et al. Structural dynamics and topology of phospholamban in oriented lipid bilayers using multidimensional solid-state NMR. Biochemistry. 2006; 45(46):13827–34. [PubMed: 17105201]
2. Fleissner MR, et al. Structure and dynamics of a conformationally constrained nitroxide side chain and applications in EPR spectroscopy. Proceedings of the National Academy of Sciences of the United States of America. 2011; 108(39):16241–6. [PubMed: 21911399]
3. Durr UH, Soong R, Ramamoorthy A. When detergent meets bilayer: birth and coming of age of lipid bicelles. Progress in nuclear magnetic resonance spectroscopy. 2013; 69:1–22. [PubMed: 23465641]
4. Vostrikov VV, et al. Structural dynamics and topology of phosphorylated phospholamban homopentamer reveal its role in the regulation of calcium transport. Structure. 2013; 21(12):2119–30. [PubMed: 24207128]
5. McCaffrey JE, James ZM, Thomas DD. Optimization of bicelle lipid composition and temperature for EPR spectroscopy of aligned membranes. Journal of magnetic resonance. 2015; 250:71–5. [PubMed: 25514061]
6. Karim CB, et al. Phospholamban structural dynamics in lipid bilayers probed by a spin label rigidly coupled to the peptide backbone. Proc Natl Acad Sci U S A. 2004; 101(40):14437–42. [PubMed: 15448204]
7. Ghimire H, et al. Probing the helical tilt and dynamic properties of membrane-bound phospholamban in magnetically aligned bicelles using electron paramagnetic resonance spectroscopy. Biochimica et biophysica acta. 2012; 1818(3):645–50. [PubMed: 22172806]
8. Karim CB, et al. Phosphorylation-dependent Conformational Switch in Spin-labeled Phospholamban Bound to SERCA. J Mol Biol. 2006; 358(4):1032–40. [PubMed: 16574147]
9. Li J, et al. Structural and functional dynamics of an integral membrane protein complex modulated by lipid headgroup charge. J Mol Biol. 2012; 418(5):379–89. [PubMed: 22381409]

10. Nesmelov YE, et al. Rotational dynamics of phospholamban determined by multifrequency electron paramagnetic resonance. Biophys J. 2007; 93(8):2805–12. [PubMed: 17573437]
11. James ZM, et al. Protein-protein interactions in calcium transport regulation probed by saturation transfer electron paramagnetic resonance. Biophys J. 2012; 103(6):1370–8. [PubMed: 22995510]
12. Inbaraj JJ, et al. Determining the topology of integral membrane peptides using EPR spectroscopy. Journal of the American Chemical Society. 2006; 128(29):9549–54. [PubMed: 16848493]
13. Karp ES, et al. The structural properties of the transmembrane segment of the integral membrane protein phospholamban utilizing (13)C CPMAS, (2)H, and REDOR solid-state NMR spectroscopy. Biochimica et biophysica acta. 2006; 1758(6):772–80. [PubMed: 16839519]
14. Torres J, Adams PD, Arkin IT. Use of a new label, (13)==(18)O, in the determination of a structural model of phospholamban in a lipid bilayer. Spatial restraints resolve the ambiguity arising from interpretations of mutagenesis data. Journal of molecular biology. 2000; 300(4):677–85. [PubMed: 10891262]
15. Bortolus M, et al. Alamethicin in bicelles: orientation, aggregation, and bilayer modification as a function of peptide concentration. Biochim Biophys Acta. 2013; 1828(11):2620–7. [PubMed: 23860254]
16. Thompson AR, et al. Bifunctional spin labeling of muscle proteins: accurate distance, orientation, and rotational dynamics by EPR. Methods in Enzymology. 2015 in press.
17. Moen RJ, Thomas DD, Klein JC. Conformationally trapping the actin-binding cleft of myosin with a bifunctional spin label. J Biol Chem. 2013; 288(5):3016–24. [PubMed: 23250750]
18. Thompson AR, et al. Structural dynamics of the actomyosin complex probed by a bifunctional spin label that cross-links SH1 and SH2. Biophys J. 2008; 95(11):5238–46. [PubMed: 18805936]
19. Arata T, et al. Orientation and motion of myosin light chain and troponin in reconstituted muscle fibers as detected by ESR with a new bifunctional spin label. Advances in experimental medicine and biology. 2003; 538:279–83. discussion 284. [PubMed: 15098675]
20. Mello RN, Thomas DD. Three distinct actin-attached structural states of myosin in muscle fibers. Biophys J. 2012; 102(5):1088–96. [PubMed: 22404931]
21. Binder BP, et al. High-resolution helix orientation in actin-bound myosin determined with a bifunctional spin label. Proceedings of the National Academy of Sciences of the United States of America. 2015
22. Sahu ID, et al. DEER EPR measurements for membrane protein structures via bifunctional spin labels and lipodisq nanoparticles. Biochemistry. 2013; 52(38):6627–32. [PubMed: 23984855]
23. Li Q, et al. Structural basis of lipid-driven conformational transitions in the KvAP voltage-sensing domain. Nat Struct Mol Biol. 2014; 21(2):160–6. [PubMed: 24413055]
24. MacLennan DH, Kranias EG. Phospholamban: a crucial regulator of cardiac contractility. Nature reviews Molecular cell biology. 2003; 4(7):566–77. [PubMed: 12838339]
25. Traaseth NJ, et al. Spectroscopic validation of the pentameric structure of phospholamban. Proc Natl Acad Sci U S A. 2007; 104(37):14676–81. [PubMed: 17804809]
26. Mascioni A, et al. Solid-state NMR and rigid body molecular dynamics to determine domain orientations of monomeric phospholamban. Journal of the American Chemical Society. 2002; 124(32):9392–3. [PubMed: 12167032]
27. Mascioni A, et al. Solid-state NMR and rigid body molecular dynamics to determine domain orientations of monomeric phospholamban. J Am Chem Soc. 2002; 124(32):9392–3. [PubMed: 12167032]
28. Buck B, et al. Overexpression, purification, and characterization of recombinant Ca-ATPase regulators for high-resolution solution and solid-state NMR studies. Protein Expr Purif. 2003; 30(2):253–61. [PubMed: 12880775]
29. Blommel PG, Fox BG. A combined approach to improving large-scale production of tobacco etch virus protease. Protein Expr Purif. 2007; 55(1):53–68. [PubMed: 17543538]
30. Douglas JL, et al. Rapid, high-yield expression and purification of Ca2+-ATPase regulatory proteins for high-resolution structural studies. Protein Expr Purif. 2005; 40(1):118–25. [PubMed: 15721779]
31. Veglia G, et al. What can we learn from a small regulatory membrane protein? Methods Mol Biol. 2010; 654:303–19. [PubMed: 20665273]

32. Cho HS, Dominick JL, Spence MM. Lipid domains in bicelles containing unsaturated lipids and cholesterol. The journal of physical chemistry B. 2010; 114(28):9238–45. [PubMed: 20583789]
33. Earle KA, Budil DE. Calculating slow-motion ESR spectra of spin-labeled polymers. 2006; 3 Chapter.
34. Traaseth NJ, et al. Structure and topology of monomeric phospholamban in lipid membranes determined by a hybrid solution and solid-state NMR approach. Proc Natl Acad Sci U S A. 2009; 106(25):10165–70. [PubMed: 19509339]
35. Brooks BR, et al. CHARMM: the biomolecular simulation program. Journal of computational chemistry. 2009; 30(10):1545–614. [PubMed: 19444816]
36. Patel S, Mackerell AD Jr, Brooks CL 3rd. CHARMM fluctuating charge force field for proteins: II protein/solvent properties from molecular dynamics simulations using a nonadditive electrostatic model. Journal of computational chemistry. 2004; 25(12):1504–14. [PubMed: 15224394]
37. Durer ZA, et al. Structural states and dynamics of the D-loop in actin. Biophys J. 2012; 103(5): 930–9. [PubMed: 23009842]
38. Budil DE, et al. Nonlinear-least-squares analysis of slow-motion EPR spectra in one and two dimensions using a modified Levenberg-Marquardt algorithm. Journal of Magnetic Resonance Series A. 1996; 120(2):155–189.
39. Columbus L, et al. Molecular motion of spin labeled side chains in alpha-helices: analysis by variation of side chain structure. Bio-chemistry. 2001; 40(13):3828–46.

Appendix A. Supplementary material

Supplementary data associated with this article can be found, in the online version, at <INSERT_WEB_ADDRESS_HERE>.

Highlights

- Bifunctional spin labels attach rigidly and stereospecifically to proteins.
- Monofunctional spin labels do not.
- Accurate orientation measurements require rigid and stereospecific spin labels.
- Molecular dynamics simulations determine spin label conformation on proteins.
- EPR and MD synergize to produce accurate phospholamban structural data.

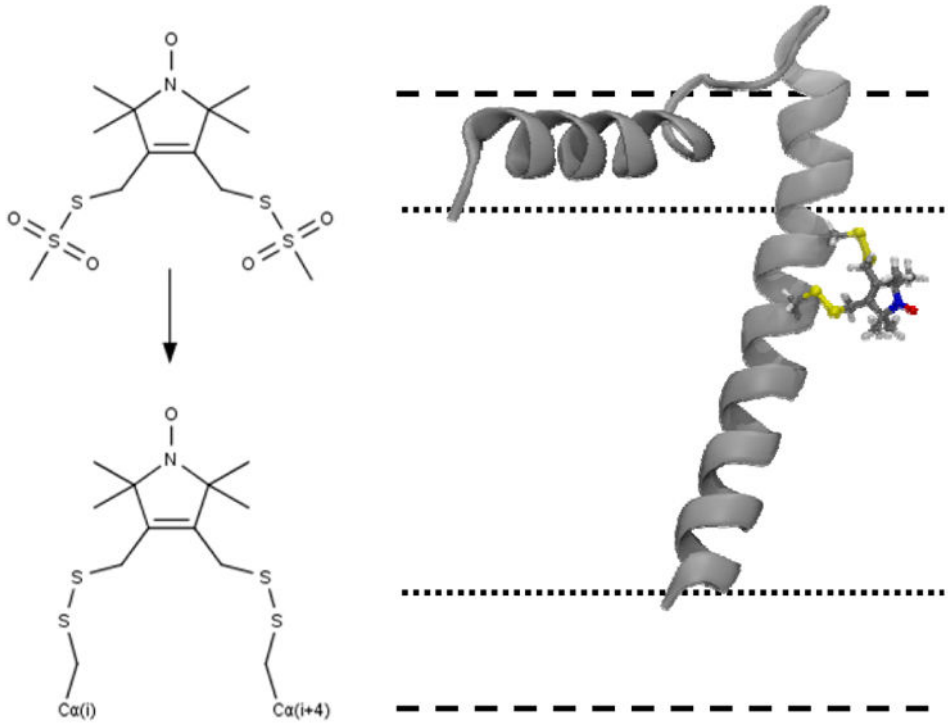

Figure 1.

Left: structural formula of BSL before and after reaction. Right: energy-minimized structure of BSL attached to Cys at positions 32 and 36 on monomeric PLB, based on the NMR structure [1]. BSL dihedral angles were initialized from an x-ray crystal structure of BSL attached to a helix on T4 lysozyme [2], then further refined by molecular dynamics simulations to produce the shown structure. The bilayer normal is indicated by **n**, the bilayer surface by dashed lines, and dotted lines indicate the approximate boundaries of the hydrophobic interior.

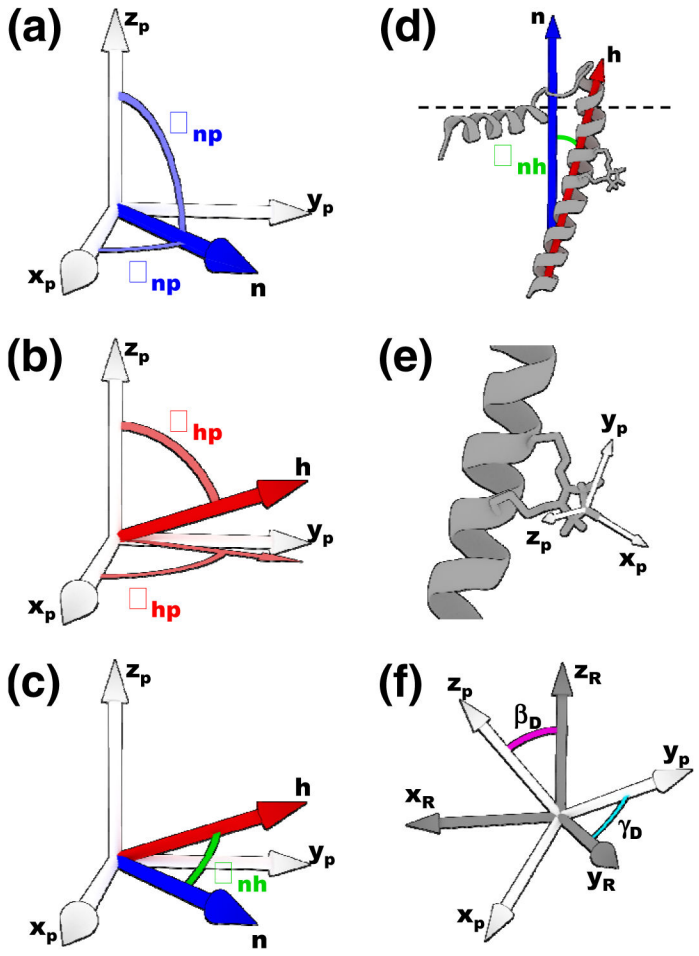

Figure 2.

BSL nitroxide coordinate system (**x**$_p$, **y**$_p$, **z**$_p$) with membrane normal (**n**) and helix long axis (**h**) vectors. (a) The membrane normal is described by the spherical angles θ_{np} and φ_{np}. (b) The helix long axis is described by the spherical angles θ_{hp} and φ_{hp}. (c) θ_{nh} is the angle spanning **n** to **h**, the PLB transmembrane helix tilt relative to the normal (d). (e) Closeup of the nitroxide coordinate system superimposed on the nitroxide structure. (f) Euler rotation (z-y-z convention) with diffusion tilt angles β_D and γ_D used to transform the principal diffusion axis (z_R = n) into the probe coordinate system shown in (a) [33].

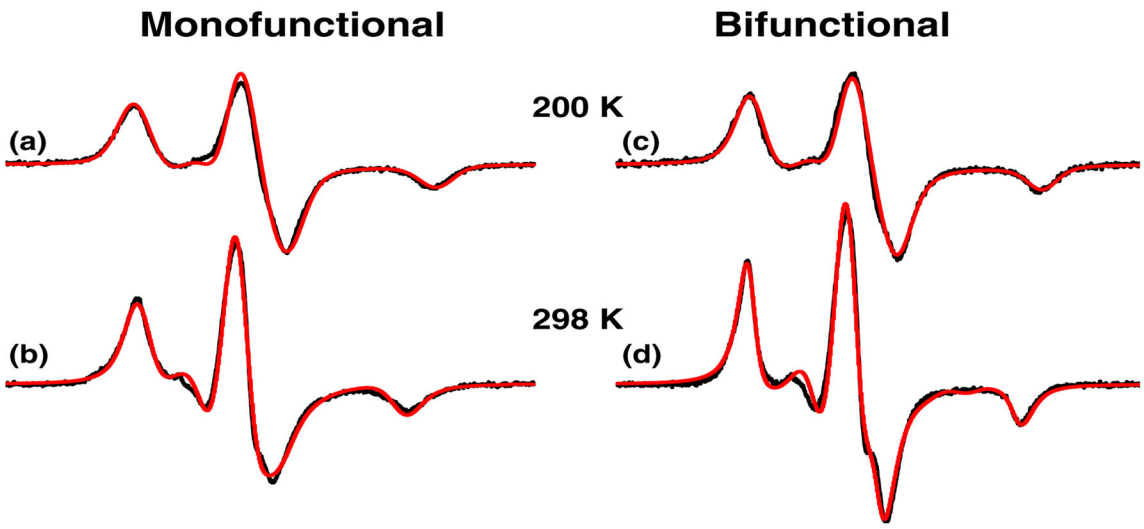

Figure 3.

EPR spectra (black) of monofunctional 32-BSL-PLB (left) and bifunctional 32/36-BSL-PLB (right) in randomly-oriented lipid vesicles at 200 K (top) and 298 K (bottom), with best fits (red) for rigid-limit (200 K) and MOMD (298 K) models (parameters from fits in Table 1). Sweep width on horizontal axis is 120 G.

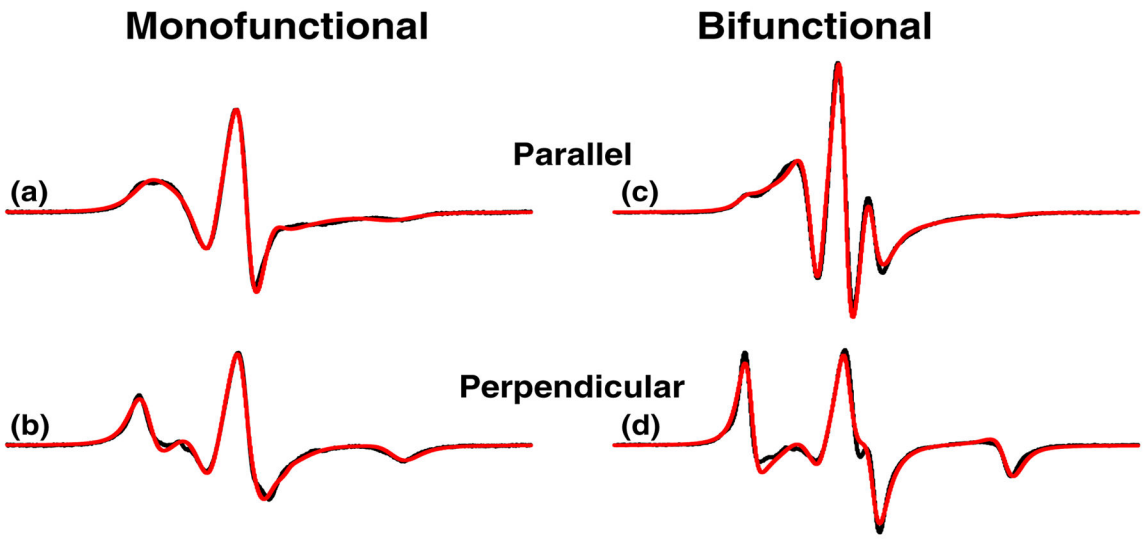

Figure 4.

EPR spectra (black) of monofunctional 32-BSL-PLB (left) and bifunctional 32/36-BSL-PLB (right) in bicelles with the membrane normal aligned parallel (top) and perpendicular (bottom) with respect to the applied magnetic field. Best fits (red) correspond to global analysis of (a) and (b) or (c) and (d). Parameter values from fits are in Table 1. Spectra were acquired at 298 K, and sweep width on horizontal axis is 120 G.

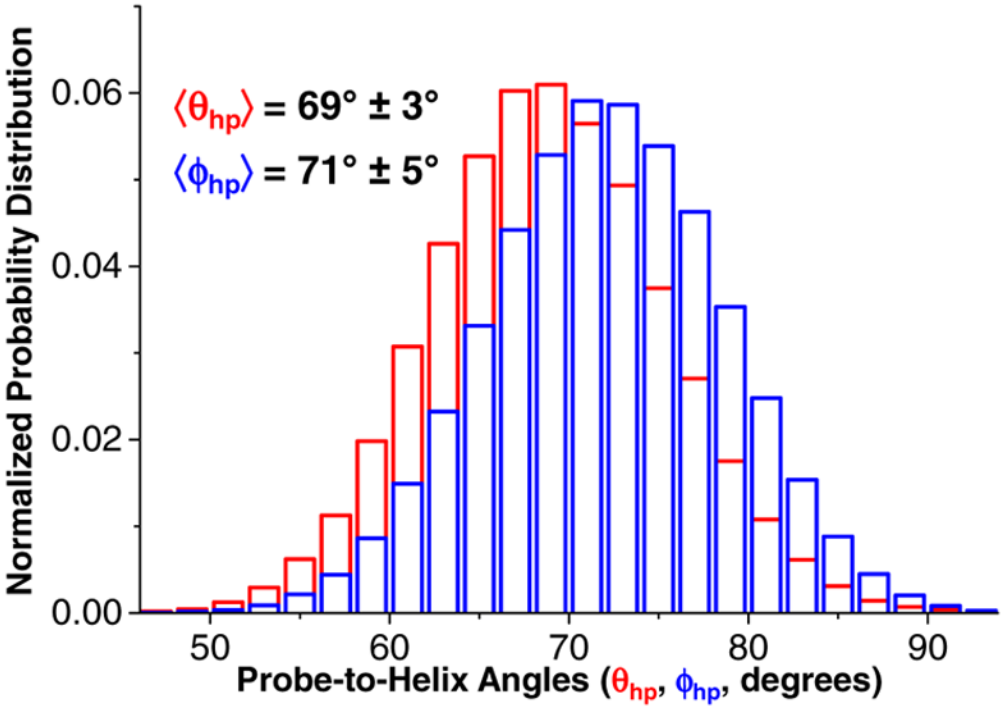

Figure 5.

Distribution for angles between nitroxide principal axis and PLB long helix axis (θ_{hp} and φ_{hp}) reported by molecular dynamics simulation of BSL modeled at positions 32 and 36 of the transmembrane helix. Peak values and associated uncertainties shown as inset text.

Table 1

Parameters include electron *g* tensor (g), hyperfine tensor (A), rotational correlation time (τ_R), first order spherical harmonic coefficient for orienting potential (C_{20}), order parameter (S), and Euler diffusion tilt angles (β_D and γ_D). 200 K fits were determined using a rigid limit model, while 298 K fits were determined using a MOMD model.

Sample	Temp (K)	g_x	g_y	g_z	$A_{\|}$(G)	$A_{\perp}$(G)	τ_R (ns)	C_{20} (kT)	S	β_D (°)	γ_D (°)
32-BSL-PLB Vesicle	200	2.00865 ± 0.00028	2.00654 ± 0.00032	2.00212 ± 0.00045	33.27 ± 0.33	5.78 ± 0.31	-	-	-	-	-
32/36-BSL-PLB Vesicle	200	2.00866 ± 0.00024	2.00641 ± 0.00039	2.00228 ± 0.00031	33.89 ± 0.65	5.92 ± 0.32	-	-	-	-	-
32-BSL-PLB Vesicle	298	2.00877 ± 0.00023	2.00611 ± 0.00051	2.00184 ± 0.00048	33.16 ± 0.50	5.49 ± 0.11	16.7 ± 1.1	1.7 ± 0.4	0.37 ± 0.09	-	-
32/36-BSL-PLB Vesicle	298	2.00843 ± 0.00022	2.00647 ± 0.00014	2.00225 ± 0.00031	32.52 ± 0.32	5.71 ± 0.09	76.2 ± 2.2	2.6 ± 0.4	0.55 ± 0.07	-	-
32-BSL-PLB Bicelle	298	2.00867 ± 0.00032	2.00597 ± 0.00057	2.00174 ± 0.00060	33.16 ± 0.27	5.48 ± 0.25	10.8 ± 0.8	1.8 ± 0.2	0.39 ± 0.04	62 ± 19	48 ± 34
32/36-BSL-PLB Bicelle	298	2.00866 ± 0.00029	2.00655 ± 0.00029	2.00211 ± 0.00033	31.76 ± 0.19	5.59 ± 0.11	70.5 ± 4.1	2.8 ± 0.3	0.57 ± 0.05	90 ± 3	62 ± 20

Table 2

BSL orientation comparison utilizing EPR, NMR, MD, and x-ray crystallography data. Row 1: PLB transmembrane helix tilt determined by EPR using MD probe conformation, as compared to NMR data [1]. Row 2: BSL diffusion tilt angle determined by EPR, as compared to molecular dynamics simulations. Row 3: BSL principal axis tilt relative to the helix axis determined by molecular dynamics simulations (MD), as compared to the crystal structure of a BSL-labeled helix in T4 lysozyme [2].

PLB TM Helix Tilt (θ_{nh})	21.8° ± 2° (EPR + MD)	21° ± 2° (NMR)
Diffusion Tilt Angle (β_D)	90° ± 3° (EPR)	89° ± 2° (MD)
Probe-to-Helix Tilt (θ_{hp})	69° ± 3° (MD)	~75° (XTAL)